Solitary wave solutions of the conformable space–time fractional coupled diffusion equation

K. Manikandan [a],*, N. Serikbayev [b], D. Aravinthan [a], K. Hosseini [c,d]

[a] Center for Computational Modeling, Chennai Institute of Technology, Chennai 600 069, Tamilnadu, India
[b] Department of General and Theoretical Physics, L. N. Gumilyov Eurasian National University, Astana, 010008, Kazakhstan
[c] Department of Mathematics, Near East University TRNC, Mersin 10, Nicosia 99138, Turkey
[d] Department of Computer Science and Mathematics, Lebanese American University, Beirut, Lebanon

ARTICLE INFO

ABSTRACT

In the realm of spatio-temporal fractional dynamics in a predator–prey system, we investigate fractional solitary wave-like solutions using the conformable space–time fractional coupled diffusion equation. To achieve this goal, we utilize the fractional derivative wave transformation approach to convert the conformable space–time fractional coupled nonlinear partial differential equations into equivalent ordinary differential equations. Subsequently, employing the $\left(\frac{G'}{G}\right)$ expansion technique, we obtain exact solutions for the transformed coupled ordinary differential equations. With the aid of these solutions and the fractional wave transformation, we construct three distinct fractional solitary wave-like solutions, namely kink-type, periodic, and rational for the considered fractional diffusive predator–prey model. Furthermore, we explore the dynamic attributes of prey and predator population densities by manipulating the space and time fractional-order parameters. Our findings reveal a significant insight: an increase in the fractional order can lead to system stabilization and foster the coexistence of both prey and predator species.

1. Introduction

In biology and computational ecology, the significance of interactions between predator and prey species is widely recognized. When it comes to modeling, numerous factors influence the overall dynamics of a predator–prey system,[1–5] including birth, the predator's attack potency, death, delayed maturation, and more. In addition, the functional response is recognized as a crucial factor in elucidating interactions between prey and predator populations. Over recent decades, various functional responses have been developed to explore and characterize specific interactions between the species under examination.[6–9] An intriguing aspect involves the exploration of spatial distribution patterns using diffusion models, even in the absence of environmental heterogeneity.[10–14] The establishment of explicit solutions is vital for gaining a deeper understanding of the underlying processes.

On account of the variability of populations and environments, the fractional prey–predator system containing diffusion is of considerable significance.[6–8,14,15] This fractional diffusive predator–prey (DPP) equation is extremely significant, so a lot of researchers have become intrigued by identifying analytical solutions to it. As a result, numerous integration tools have been used to acquire this equation's wave solutions. Recently, utilizing two different kinds of fractional derivatives,

conformable and Caputo, wave solutions to the time-fractional DPP model have been studied.[16] One novel fractional-order DPP model with group defense is proposed in,[6] for example, using the Caputo fractional derivative. Aside from their physical significance, close-form solutions for partial differential equations that are nonlinear aid numerical solvers in stability analysis by allowing them to compare the preciseness of the outcomes.[8,9,17] An attempt has been developed an efficient numerical solution for computing the predator–prey model's functional response (Beddington–DeAngelis) and fractional derivatives with a Mittag-Leffler kernel.[17] In Ref. [8], a variation of the Kolmogorov model called the Gauss-type predator–prey model was investigated. This model included the Allee effect and the Holling type-III functional response. In Ref. [15], a novel formulation of a spatial predator–prey model, incorporating Leslie–Gower and Holling type II schemes in the context of prey social behavior, has been systematically investigated. The study explores the impact of predator harvesting on predator–prey interactions in the presence of prey social behavior, employing a reaction–diffusion system subjected to Neumann boundary conditions.[18] Additionally, the asymptotic analysis of spatially heterogeneous viral transmission, considering cell-to-cell transmission, virus nonlocal dispersal, and intracellular delay, has been examined.[19]

Furthermore, the global threshold dynamics of a hybrid viral infection model has been studied, assuming all parameters are spatially dependent. The study establishes the existence and uniqueness of a global solution, demonstrating the presence of a global compact attractor.[20]

The study and modeling of a wide range of phenomena in various fields have significantly benefited from the framework of nonlinear fractional partial differential equations (NFPDEs).[21-26] Due to the complexity of the fractional calculus, there are no exact analytical procedures that can provide exact results for NFPDEs. Establishing reliable and consistent numerical and analytical techniques for solving physically and biologically relevant FPDEs has also required a lot of research. However, many computational and analytical approaches were developed as a result of the pursuit for reliable fractional solutions in various investigations,[16,25,27-32] such as fractional sub-equation, Sine–Gordon expansion, first integral, variational iteration, exponential function techniques, and so on. It is ultimately of significant interest to investigate fractional derivative partial differential equations and look for their solitary wave solutions because of the vital role of solitary waves in numerous fields of research.[33-38]

In addition to established fractional derivative definitions such as Riemann–Liouville, Caputo, He, local, and Grunwald–Letnikov for NFPDEs,[25,26] Khalil et al. introduced a novel and straightforward definition known as the conformable fractional derivative.[39] This new definition has garnered considerable interest among mathematicians and physicists. More recently, Abdon Atangana proposed the beta-derivative as an extension of these fractional derivatives.[40] While the aforementioned derivatives can be seen as a logical progression from classical derivatives rather than fractional derivatives, Chen introduced a fractal derivative based on the fractal paradigm.[41] In recent decades, research on fractal derivatives has flourished due to their intriguing properties. Moreover, fractal derivatives offer a more accessible means to theoretically investigate certain physical models. A notable advantage of fractal derivatives is their ability to be straightforwardly transformed into their traditional form using transformation analogues akin to fractional complex transforms.[42] Consequently, a novel (3+1)-dimensional modified Zakharov–Kuznetsov equation, incorporating the conformable fractional derivative, has been formulated.[43] Using an innovative approach known as the fractal semi-inverse variational method, several new types of fractal traveling wave solutions have been successfully derived.[43] The modified KdV–Zakharov–Kuznetsov equation has been subject to a fractal modification, and its fractal generalized variational structure has been established through the semi-inverse method.[44] Moreover, a new fractal modified equal width-Burgers equation, involving the local fractional derivative, has been derived.[45] Utilizing the Mittag-Leffler function method, traveling wave solutions for this equation have been obtained. In addition to this, significant efforts have been directed towards deriving localized solutions for fractional nonlinear Schrödinger-type equations.[17,30,32,35,37]

In the development of the above stated investigations, in this work, we focus on the fractional two-coupled partial differential equations that model the population dynamics of prey and predator, where the fractional derivative is defined in the sense of conformable. We here intend to study the solitary wave dynamics in this model. For this, we transform the model under investigation into two coupled ODEs through fractional derivative wave transformation. We construct two sets of three different solitary wave-like solutions, namely kink type, periodic, and rational, for the later equation by utilizing the $\left(\frac{G'}{G}\right)$ expansion method. We then show the dynamical nature of solitary-like profiles in three different situations. Furthermore, we also investigate the impact of the fractional order on the dynamics of the prey–predator model. We find that the fractional order/derivative power affect the stability and behavior of the population dynamics. Specifically, we observe that the fractional order plays a significant role in determining the coexistence or extinction of the prey and predator species. In accordance with our findings, increasing the fractional order may regulate the system while favoring the cohabitation of predator and prey species.

The structure of the paper is as follows. In Section 2, we consider the conformable space–time fractional DPP model and construct the solitary wave solutions through the $\left(\frac{G'}{G}\right)$ expansion method. We then obtain three different solitary wave solutions, namely kink-type, periodic, and rational, for two different wave velocities. Furthermore, we also investigate the dynamical features of the considered model by varying the space-fractional and time-fractional derivative power parameters. Finally, we conclude our findings in Section 3.

2. Fractional diffusive predator–prey model and its solitary-wave like solutions

The fractional coupled diffusion equation is a mathematical model that extends classical diffusion equations by incorporating fractional derivatives. It is used to describe the dynamics of multiple entities undergoing diffusion in a system, where the movement of particles is influenced not only by their immediate surroundings but also by historical positions and interactions.[2-4] The fractional derivatives introduce memory and non-locality into the model, allowing for a more accurate representation of complex diffusion processes. This equation finds applications in various scientific fields, including physics, biology, and materials science, where multi-scale modeling and the characterization of anomalous diffusion behavior are essential. Numerical simulations and analytical techniques are employed to solve the fractional coupled diffusion equation, revealing emergent phenomena and providing insights into the intricate dynamics of diffusing entities in complex systems.[10,11] Considering these advancements in fractional coupled diffusion phenomena, this study investigates the conformable space–time fractional diffusive predator–prey system.

In this work, we consider the conformable space–time fractional diffusive predator–prey (CSTFPP) system, which is of the form

$$\phi_{1t}^{\mu} = \phi_{1xx}^{\lambda} - s\phi_1 + (1+s)\phi_1^2 - \phi_1^3 - \phi_1\phi_2,$$
$$\phi_{2t}^{\mu} = \phi_{2xx}^{\lambda} + r\phi_1\phi_2 - b\phi_2 - \delta\phi_2^3, \tag{2.1}$$

where $\phi_1 = \phi_1(x,t)$ and $\phi_2 = \phi_2(x,t)$ denote the prey and predator densities, respectively. The derivative D_t^{μ} is the time-fractional and D_{xx}^{λ} is the space-fractional derivative, where λ and μ $(0 < \mu, \lambda \leq 1)$ represent the space and time-fractional order parameter/derivative power. The parameters s, δ, r and b are positive constants. The biological interpretation of Eq. (2.1) and the presence of parameters has been explained in-detail, one may refer.[4,5] In order to explore the dynamical characteristics of the model (2.1), we convert the above mentioned model into the following system by presuming the connections between the parameters $(b = s$ and $r + \frac{1}{\sqrt{\delta}} = s + 1)$, that is

$$\phi_{1t}^{\mu} = \phi_{1xx}^{\lambda} - s\phi_1 + (r + \frac{1}{\sqrt{\delta}})\phi_1^2 - \phi_1^3 - \phi_1\phi_2$$
$$\phi_{2t}^{\mu} = \phi_{2xx}^{\lambda} + r\phi_1\phi_2 - s\phi_2 - \delta\phi_2^3. \tag{2.2}$$

It is noticed that numerous features of the predator–prey system have been investigated by constructing traveling, kink-type, and periodic wave solutions through different integration schemes,[4,5,46-48] when μ and λ are equal to one.

Next, we intend to study the impact of space and time fractional-order parameters on the solitary wave solutions, we first derive them in the considered model (2.2). For this, we adopt the fractional derivative wave transformation to the CSTFDPP system. The following definition and properties are pertinent to this study[39,40,42]:

Definition. For a function $g : (0, \infty] \to \mathbb{R}$, the conformable fractional derivative of g of order μ is defined by

$$D_t^{\mu} g(t) = \lim_{\epsilon \to 0} \frac{g(t + \epsilon t^{1-\mu}) - g(t)}{\epsilon}. \tag{2.3}$$

These newly defined fractional derivative has a number of well-known features, including:

Let $\mu \in (0,1]$ and k, l be the μ differentiable at point $t > 0$, then we have

- $g_\mu(ak + dl) = d\, g_\mu(k) + d\, g_\mu(l), \forall a, d \in \mathbb{R}.$
- $g_\mu(t^q) = qt^{q-\mu}, \forall q \in \mathbb{R}.$
- $g_\mu(a) = 0$, for all constant $k(t) = a.$
- $g_\mu(kl) = k\, g_\mu(l) + l\, g_\mu(k).$
- $g_\mu\left(\frac{k}{l}\right) = \frac{l\, g_\mu(k) - k\, g_\mu(l)}{l^2}.$
- If, in addition to k is differentiable, then $g_\mu(k)(t) = t^{1-\mu}\frac{dk}{dt}.$

By considering the above-mentioned definition and properties with the fractional derivative wave transformation, we first convert the CSTFDPP Eqs. (2.2) into its traditional form. To do so, we consider the transformation[30,39,42] as

$$\phi_1(x,t) = \phi_1(\xi), \quad \phi_2(x,t) = \phi_2(\xi), \qquad \xi = \frac{x^\lambda}{\lambda} - c\frac{t^\mu}{\mu}. \tag{2.4}$$

Plugging this transformation (2.4) into CSTFDPP Eqs. (2.2), we arrive

$$\phi_1'' + c\phi_1' - s\phi_1 + \left(r + \frac{1}{\sqrt{\delta}}\right)\phi_1^2 - \phi_1^3 - \phi_1\phi_2 = 0,$$

$$\phi_2'' + c\phi_2' + r\phi_1\phi_2 - s\phi_2 - \delta\phi_2^3 = 0. \tag{2.5}$$

It is essential to highlight that the two coupled ordinary differential Eqs. (2.5) can be investigated through various analytical methods discussed in the introduction section. Among the available analytical approaches, we opt for the $\left(\frac{G'}{G}\right)$-expansion method to solve Eqs. (2.5) due to its simplicity and efficiency. By applying this method to (2.5), we consider a polynomial in $\left(\frac{G'}{G}\right)$ of the following form:

$$\phi_1(\xi) = p_m\left(\frac{G'}{G}\right)^m + p_{m-1}\left(\frac{G'}{G}\right)^{m-1} + p_{m-2}\left(\frac{G'}{G}\right)^{m-2} + \cdots,$$

$$\phi_2(\xi) = q_n\left(\frac{G'}{G}\right)^n + q_{n-1}\left(\frac{G'}{G}\right)^{n-1} + q_{n-2}\left(\frac{G'}{G}\right)^{n-2} + \cdots, \tag{2.6}$$

with $G = G(\xi)$ denotes the solution of the following equation as

$$G'' + \alpha G' + \beta G = 0. \tag{2.7}$$

In Eqs. (2.6) and (2.7), the parameters p_m, p_{m-1}, p_{m-2}, q_n, q_{n-1}, q_{n-2}, α and β are constants which can be calculated below. To determine the values of m and n, we substitute the presumed solutions (2.6) into Eq. (2.5). After simplifying the yield equation, we determine that $m = 1$ and $n = 1$. Considering these values in (2.6), they are reduced in the following equations, such as

$$\phi_1(\xi) = p_1\left(\frac{G'}{G}\right) + p_0, \quad \phi_2(\xi) = q_1\left(\frac{G'}{G}\right) + q_0, \quad p_1, q_1 \neq 0. \tag{2.8}$$

Substituting the above expressions (2.8) and their first and second order derivatives in (2.5), we come up with the following equations with $G''(\xi)$ and $G'''(\xi)$, that is

$$\frac{p_1 G'(\xi)\left(G'(\xi)\left(p_1\left(-3\sqrt{\delta}p_0 + \sqrt{\delta}r + 1\right) - \sqrt{\delta}(c + q_1)\right) - 3\sqrt{\delta}G''(\xi)\right)}{\sqrt{\delta}G(\xi)^2}$$

$$+ \frac{p_1\left(cG''(\xi) + G^{(3)}(\xi)\right) + G'(\xi)\left(2kp_1p_0 + p_0\left(\frac{2p_1}{\sqrt{\delta}} - q_1\right) - p_1(q_0 + s) - 3p_1p_0^2\right)}{G(\xi)}$$

$$- \frac{p_1\left(p_1^2 - 2\right)G'(\xi)^3}{G(\xi)^3} + p_0\left(kp_0 + \frac{p_0}{\sqrt{\delta}} - p_0^2 - q_0 - s\right) = 0, \tag{2.9}$$

$$\frac{G'(\xi)\left(p_0q_1r + p_1q_1r - 3\delta q_1^3 - q_1 s\right)}{G(\xi)} + \frac{G'(\xi)^2\left(p_1q_1r - 3\delta q_1^3\right)}{G(\xi)^2}$$

$$- \frac{cq_1 G'(\xi)^2}{G(\xi)^2} + \frac{cq_1 G''(\xi)}{G(\xi)} - \frac{\delta q_1^3 G'(\xi)^3}{G(\xi)^3} - \frac{2q_1 G'(\xi)G''(\xi)}{G(\xi)^2} + \frac{q_1 G^{(3)}(\xi)}{G(\xi)}$$

$$+ q_1 G'(\xi)\left(\frac{2G'(\xi)^2}{G(\xi)^3} - \frac{G''(\xi)}{G(\xi)^2}\right) + p_0q_1r - \delta q_1^3 - q_1 s = 0. \tag{2.10}$$

By replacing $G''(\xi) = -\alpha G'(\xi) - \beta G(\xi)$ and $G^{(3)}(\xi) = \alpha^2 G'(\xi) + \alpha\beta G(\xi) - \mu G'(\xi)$ in the above equations and reorganizing with different powers of $\left(\frac{G'}{G}\right)$, we obtain

$$[2p_1 - p_1^3]\left(\frac{G'}{G}\right)^3 + \left[3p_1\alpha - cp_1 + rp_1^2 + \frac{p_1^2}{\sqrt{\delta}} - 3p_1^2 p_0 - p_1 q_1\right]\left(\frac{G'}{G}\right)^2$$

$$+ \left[(2\beta + \alpha^2)p_1 - c\alpha p_1 - sp_1 + 2rp_0 p_1 + \frac{2p_1 p_0}{\sqrt{\delta}} - 3p_0^2 p_1 - p_1 q_0 - p_0 q_1\right]\left(\frac{G'}{G}\right)$$

$$+ \left[\beta p_1\alpha - c\beta p_1 - sp_0 + rp_0^2 + \frac{p_0^2}{\sqrt{\delta}} - p_0^3 - p_0 q_0\right] = 0, \tag{2.11}$$

$$[2q_1 - \delta q_1^3]\left(\frac{G'}{G}\right)^3 + [3q_1\alpha - cq_1 + rp_1 q_1 - 3\delta q_1^2 q_0]\left(\frac{G'}{G}\right)^2$$

$$+ [(2\beta + \alpha^2)q_1 - c\alpha q_1 - sq_1 + rp_0 q_1 + rp_1 q_0 - 3\delta q_0^2 q_1]\left(\frac{G'}{G}\right)$$

$$+ [\beta q_1\alpha - c\beta q_1 - sq_0 + rp_0 q_0 - \delta q_0^3] = 0. \tag{2.12}$$

By setting the coefficients of different powers of $\left(\frac{G'}{G}\right)$ to zero in the Eqs. (2.11) and (2.12), we arrive the system of algebraic equations, namely

$$2p_1 - p_1^3 = 0,$$

$$3p_1\alpha - cp_1 + rp_1^2 + \frac{p_1^2}{\sqrt{\delta}} - 3p_1^2 p_0 - p_1 q_1 = 0,$$

$$(2\beta + \alpha^2)p_1 - c\alpha p_1 - sp_1 + 2rp_0 p_1 + \frac{2p_1 p_0}{\sqrt{\delta}} - 3p_0^2 p_1 - p_1 q_0 - p_0 q_1 = 0,$$

$$\beta p_1\alpha - c\beta p_1 - sp_0 + rp_0^2 + \frac{p_0^2}{\sqrt{\delta}} - p_0^3 - p_0 q_0 = 0, \tag{2.13}$$

$$2q_1 - \delta q_1^3 = 0,$$

$$3q_1\alpha - cq_1 + rp_1 q_1 - 3\delta q_1^2 q_0 = 0,$$

$$(2\beta + \alpha^2)q_1 - c\alpha q_1 - sq_1 + rp_0 q_1 + rp_1 q_0 - 3\delta q_0^2 q_1 = 0,$$

$$\beta q_1\alpha - c\beta q_1 - sq_0 + rp_0 q_0 - \delta q_0^3 = 0.$$

Two sets of constant values, namely p_1, p_0, q_1, q_0 and c are obtained by solving the sets of algebraic expressions (2.13) as

Case (i) $p_1 = \pm\sqrt{2}$, $q_0 = \frac{p_0}{\sqrt{\delta}}$, $q_1 = \pm\sqrt{\frac{2}{\delta}}$, $c = \mp\frac{r}{\sqrt{2}}$, $\alpha = \mp\frac{r - 2p_0}{\sqrt{2}}$,

$$s = kp_0 - p_0^2 + 2\beta. \tag{2.14}$$

Case (ii) $p_1 = \pm\sqrt{2}$, $q_0 = \frac{p_0}{\sqrt{\delta}}$, $q_1 = \pm\sqrt{\frac{2}{\delta}}$, $\alpha = \pm\frac{p_0^2 + 2\beta}{\sqrt{2}p_0}$, $\tag{2.15}$

$$c = \pm\frac{1}{\sqrt{2}}\left(2r - 3p_0 + \frac{6\beta}{p_0}\right), \quad s = -\frac{(p_0^2 - 2\beta)(-rp_0 + p_0^2 - 2\beta)}{p_0^2}.$$

It is verified that these four set of parameters separately satisfy the algebraic equations given in (2.13). Utilizing the above set of constants, one can derive the explicit solitary wave solutions of the fractional DPP model under investigation (2.2).

By considering the first set of constants and substituting them into the Eq. (2.8), the solutions turn out to be of the form

$$\phi_1(\xi) = \pm\sqrt{2}\left(\frac{G'}{G}\right) + p_0, \quad \phi_2(\xi) = \pm\sqrt{\frac{2}{\delta}}\left(\frac{G'}{G}\right) + \frac{p_0}{\sqrt{\delta}}, \tag{2.16}$$

where $G(\xi)$ is the solution of (2.7). With regard to the values of α and β, it is established that Eq. (2.7) admits three distinct types of solutions, such as

Case 1: $\alpha^2 - 4\beta > 0$

$$G(\xi) = e^{(-\alpha/2)\xi}\left(c_1 \sinh\frac{\sqrt{\alpha^2 - 4\beta}}{2}\xi + c_2 \cosh\frac{\sqrt{\alpha^2 - 4\beta}}{2}\xi\right), \tag{2.17}$$
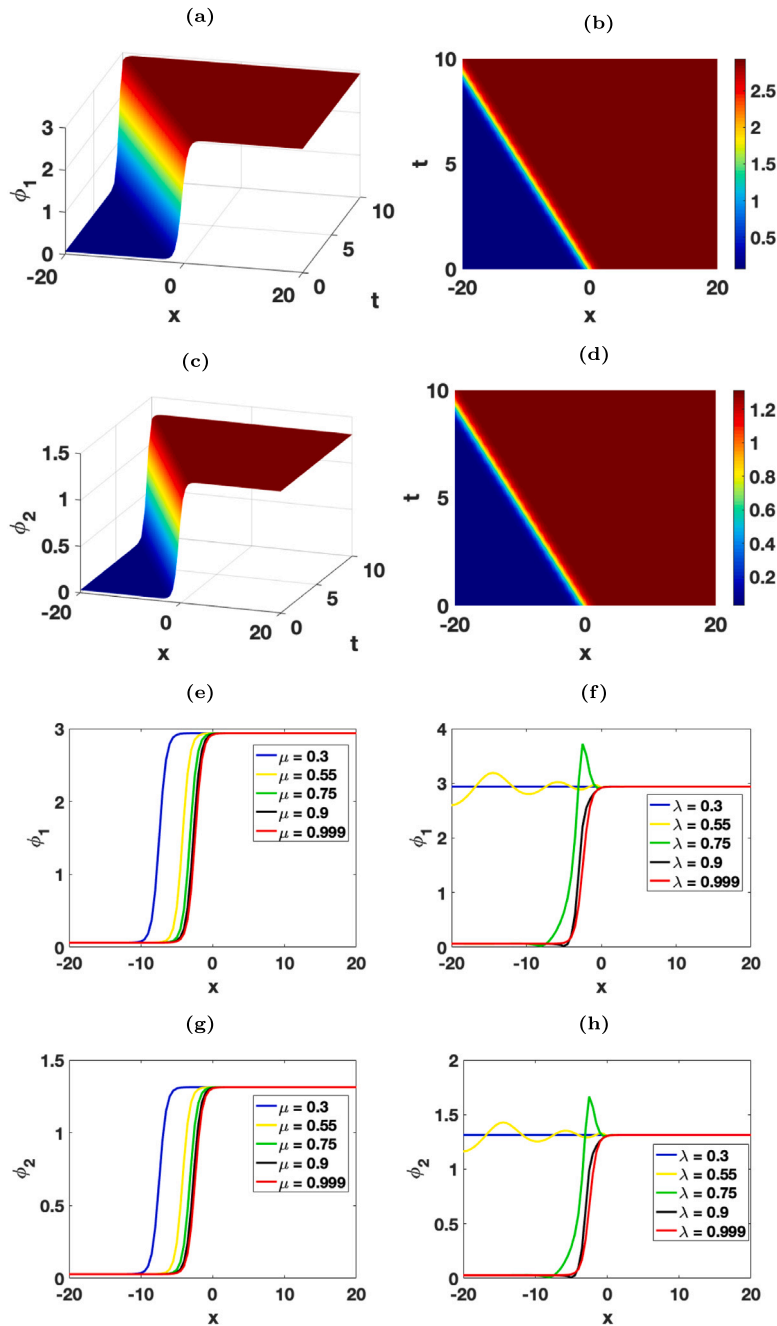
Fig. 1. Density distribution of prey (ϕ_1) and predator (ϕ_2) using the kink-like solution (2.20) for (2.2). For time and space fractional parameter $\mu = 1$ and $\lambda = 1$, (a) prey density; (b) contour plot of (a); (c) predator density; (d) contour plot of (c). (e) and (g) prey and predator density for various time-fractional parameter (μ), (f) and (h) prey and predator density for various space-fractional parameter (λ) at $t = 1$. The other parameters are $p_0 = 3.75$, $c_1 = 0.5$, $c_2 = 1.5$, $\beta = 1.5$, $\delta = 5$ and $r = 3$.

Case 2: $\alpha^2 - 4\beta < 0$

$$G(\xi) = e^{(-\alpha/2)\xi}\left(c_1 \cos \frac{\sqrt{4\beta - \alpha^2}}{2}\xi + c_2 \sin \frac{\sqrt{4\beta - \alpha^2}}{2}\xi\right), \qquad (2.18)$$

Case 3: $\alpha^2 - 4\beta = 0$

$$G(\xi) = (c_1 + c_2\xi)e^{(-\alpha/2)\xi}. \qquad (2.19)$$

When we replace (2.16) with (2.17)–(2.19), we obtain the solitary wave (kink-type, periodic and rational) solutions, namely

Case 1: kink-type solitary wave solutions when $\alpha^2 - 4\beta > 0$

$$\phi_1(\xi) = \pm\sqrt{2}\left(-\frac{\alpha}{2} + \gamma\left(\frac{c_1 \cosh\left[\gamma\left(\frac{x^\lambda}{\lambda} - c\frac{t^\mu}{\mu}\right)\right] + c_2 \sinh\left[\gamma\left(\frac{x^\lambda}{\lambda} - c\frac{t^\mu}{\mu}\right)\right]}{c_1 \sinh\left[\gamma\left(\frac{x^\lambda}{\lambda} - c\frac{t^\mu}{\mu}\right)\right] + c_2 \cosh\left[\gamma\left(\frac{x^\lambda}{\lambda} - c\frac{t^\mu}{\mu}\right)\right]}\right)\right) + p_0,$$

$$\phi_2(\xi) = \pm\sqrt{\frac{2}{\delta}}\left(-\frac{\alpha}{2} + \gamma\left(\frac{c_1 \cosh\left[\gamma\left(\frac{x^\lambda}{\lambda} - c\frac{t^\mu}{\mu}\right)\right] + c_2 \sinh\left[\gamma\left(\frac{x^\lambda}{\lambda} - c\frac{t^\mu}{\mu}\right)\right]}{c_1 \sinh\left[\gamma\left(\frac{x^\lambda}{\lambda} - c\frac{t^\mu}{\mu}\right)\right] + c_2 \cosh\left[\gamma\left(\frac{x^\lambda}{\lambda} - c\frac{t^\mu}{\mu}\right)\right]}\right)\right) + \frac{p_0}{\sqrt{\delta}}, \qquad (2.20)$$

where $\gamma = \frac{\sqrt{\alpha^2 - 4\beta}}{2}$, and $c = \mp\frac{r}{\sqrt{2}}$.

Case 2: periodic wave solution when $\alpha^2 - 4\beta < 0$

$$\phi_1(\xi) = \pm\sqrt{2}\left(-\frac{\alpha}{2} + \gamma\left(\frac{-c_1 \sin\left[\gamma\left(\frac{x^\lambda}{\lambda} - c\frac{t^\mu}{\mu}\right)\right] + c_2 \cos\left[\gamma\left(\frac{x^\lambda}{\lambda} - c\frac{t^\mu}{\mu}\right)\right]}{c_1 \cos\left[\gamma\left(\frac{x^\lambda}{\lambda} - c\frac{t^\mu}{\mu}\right)\right] + c_2 \sin\left[\gamma\left(\frac{x^\lambda}{\lambda} - c\frac{t^\mu}{\mu}\right)\right]}\right)\right) + p_0,$$
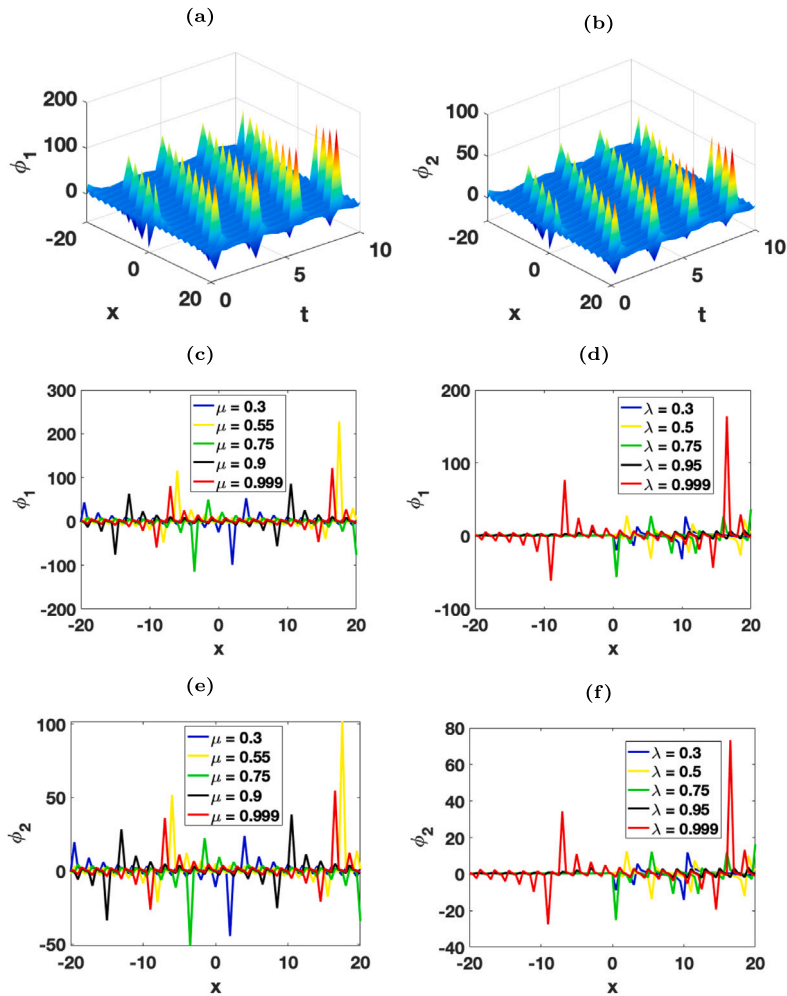
Fig. 2. Density distribution of prey (ϕ_1) and predator (ϕ_2) using the periodic wave solution (2.21) for (2.2). For $\mu = 1$ and $\lambda = 1$, (a) prey density; (b) predator density. (c) and (e) prey and predator densities for various μ, (d) and (f) prey and predator densities for various λ at $t = 1$. The other parameters are $p_0 = 1.75$, $c_1 = -0.09$, $c_2 = 2.1$, $\beta = 3$, $\delta = 5$ and $r = 1.65$.

$$\phi_2(\xi) = \pm\sqrt{\frac{2}{\delta}}\left(-\frac{\alpha}{2} + \gamma\left(\frac{-c_1\sin\left[\gamma\left(\frac{x^\lambda}{\lambda} - c\frac{t^\mu}{\mu}\right)\right] + c_2\cos\left[\gamma\left(\frac{x^\lambda}{\lambda} - c\frac{t^\mu}{\mu}\right)\right]}{c_1\cos\left[\gamma\left(\frac{x^\lambda}{\lambda} - c\frac{t^\mu}{\mu}\right)\right] + c_2\sin\left[\gamma\left(\frac{x^\lambda}{\lambda} - c\frac{t^\mu}{\mu}\right)\right]}\right)\right) + \frac{p_0}{\sqrt{\delta}},$$

$$(2.21)$$

where $\gamma = \frac{\sqrt{4\beta - \alpha^2}}{2}$, and $c = \mp\frac{r}{\sqrt{2}}$.

Case 3: rational solution when $\alpha^2 - 4\beta = 0$

$$\phi_1(\xi) = \pm\sqrt{2}\left(\frac{c_2}{c_1 + c_2\left(\frac{x^\lambda}{\lambda} - c\frac{t^\mu}{\mu}\right)} - \frac{\alpha}{2}\right) + p_0,$$

$$\phi_2(\xi) = \pm\sqrt{\frac{2}{\delta}}\left(\frac{c_2}{c_1 + c_2\left(\frac{x^\lambda}{\lambda} - c\frac{t^\mu}{\mu}\right)} - \frac{\alpha}{2}\right) + \frac{p_0}{\sqrt{\delta}},$$

$$(2.22)$$

where $p_0 = -\frac{2\sqrt{2\beta} + r}{2}$, $c = \mp\frac{r}{\sqrt{2}}$, c_1, and c_2 are arbitrary constants.

Fig. 1 shows the qualitative nature of the density of prey (ϕ_1) and predator (ϕ_2) using the fractional kink-type solitary wave solution (2.21) for CSTFDPP Eq. (2.2). We first consider the integer-order derivative case, that is, $\lambda = \mu = 1$. The kink-type solitary wave profiles are shown in Figs. 1(a) and 1(c) for prey and predator populations, respectively. The corresponding contour plots are represented in Figs. 1(b) and 1(d). We can see that density of both populations increases slowly and rapidly, and finally they reach saturation level.

The resultant profile is similar to the kink solitary wave profile. Next, we consider the fractional-derivative scenario, that is λ and $\mu < 1$. The outcomes are illustrated in Figs. 1(e)–(h). While varying the time and space-fractional derivative power, we can see the phase shift in the density profile for prey (ϕ_1) which is displayed in Figs. 1(e) and 1(f) and for predator (ϕ_1) as shown in Figs. 1(g) and 1(h), respectively. It is important to note here that we almost recover the fundamental kink-type solitary wave profile for both the parameter λ and μ approaches to unity.

In Figs. 2(a)–(b), we plot the periodic wave solution (2.21) of (2.2) for μ and λ equal to 1. These figures reveal the characteristics of the usual periodic wave profile. We then vary the fractional derivative powers (μ and λ) in the same solution (2.21). Fig. 2(c) represents the different prey densities (periodic wave profile) for different time derivative power values and fixing $\lambda = 0.99$. Also, we vary the space fractional-order parameter (μ) and fix $\mu = 0.99$, the resultant structure is demonstrated in Fig. 2(d). By varying the λ and μ values, we can attain different propagation characteristics of periodic profile in the CSTFDPP model under investigation. Similarly, we also obtain the same dynamical features in the predator density which can be visualized in Figs. 2(e)–(f).

Fig. 3 illustrates the rational/singular solitary wave profiles for prey and predator population densities using the solution (2.22). When both parameters λ and μ are fixed at 1, the typical features of a rational solitary wave profile are obtained for prey and predator density, as
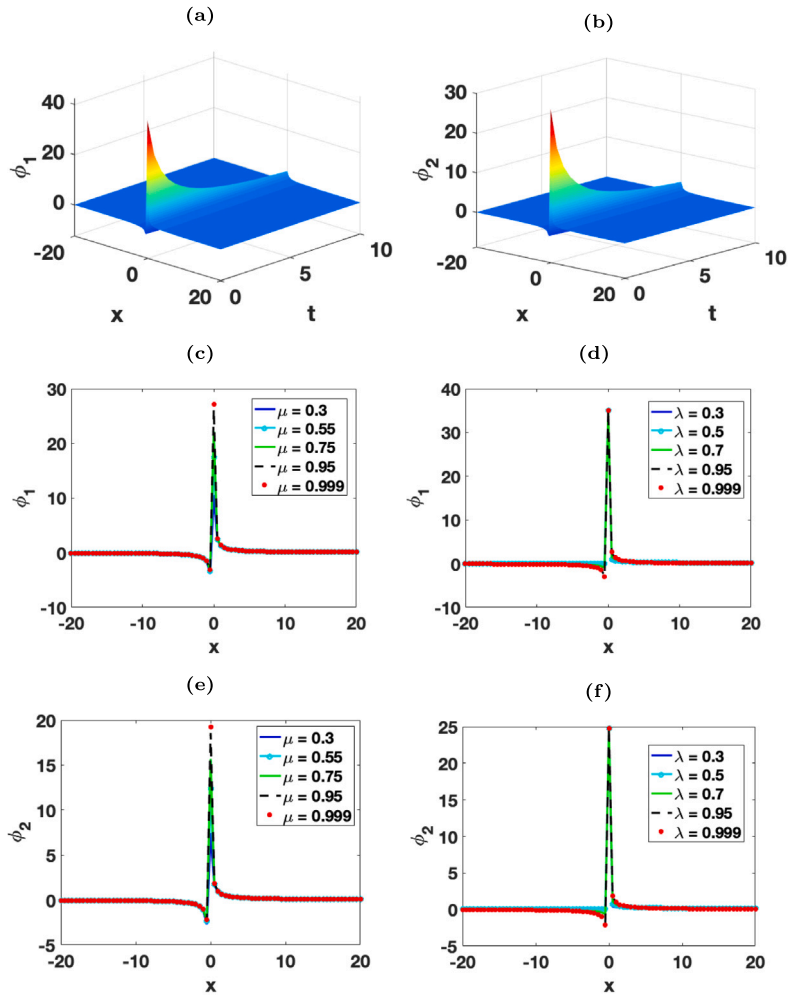
Fig. 3. Density distribution of prey (ϕ_1) and predator (ϕ_2) using the rational solution (2.22) for (1). For $\mu = 1$ and $\lambda = 1$, (a) prey density; (b) predator density. (c) and (e) prey and predator densities for various μ, (d) and (f) prey and predator densities for various λ at $t = 1$. The other parameters are $c_1 = 0.1$, $c_2 = 3$, $\beta = 3$, $\delta = 2$ and $r = 0.05$.

seen in Figs. 3(a) and (b), respectively. In the scenario where the space-fractional derivative power λ is set to 0.99 while varying the parameter μ, there are no notable changes in the resulting profiles. This observation is evident in Fig. 3(c) for prey density and Fig. 3(e) for predator density. Similarly, with $\mu = 0.99$ and varying values of λ, rational solitary wave profiles for prey and predator density are plotted, as shown in Figs. 3(d) and 3(f), respectively.

Now substituting the second set of constants (2.15) into Eq. (2.16), we get the following three traveling wave solutions (kink-type, periodic and rational) of the CSTFDPP system as

Case 1: $\alpha^2 - 4\beta > 0$

$$\phi_1(\xi) = \pm\sqrt{2}\left(-\frac{\alpha}{2}\right.$$
$$\left.+ \gamma\left(\frac{c_1 \cosh\left[\gamma\left(\frac{x^\lambda}{\lambda} - c\frac{t^\mu}{\mu}\right)\right] + c_2 \sinh\left[\gamma\left(\frac{x^\lambda}{\lambda} - c\frac{t^\mu}{\mu}\right)\right]}{c_1 \sinh\left[\gamma\left(\frac{x^\lambda}{\lambda} - c\frac{t^\mu}{\mu}\right)\right] + c_2 \cosh\left[\gamma\left(\frac{x^\lambda}{\lambda} - c\frac{t^\mu}{\mu}\right)\right]}\right)\right) + p_0,$$

$$\phi_2(\xi) = \pm\sqrt{\frac{2}{\delta}}\left(-\frac{\alpha}{2}\right.$$
$$\left.+ \gamma\left(\frac{c_1 \cosh\left[\gamma\left(\frac{x^\lambda}{\lambda} - c\frac{t^\mu}{\mu}\right)\right] + c_2 \sinh\left[\gamma\left(\frac{x^\lambda}{\lambda} - c\frac{t^\mu}{\mu}\right)\right]}{c_1 \sinh\left[\gamma\left(\frac{x^\lambda}{\lambda} - c\frac{t^\mu}{\mu}\right)\right] + c_2 \cosh\left[\gamma\left(\frac{x^\lambda}{\lambda} - c\frac{t^\mu}{\mu}\right)\right]}\right)\right) + \frac{p_0}{\sqrt{\delta}},$$

$$(2.23)$$

where $\gamma = \frac{\sqrt{\alpha^2 - 4\beta}}{2}$, and $c = \pm\frac{1}{\sqrt{2}}\left(2r - 3p_0 + \frac{6\beta}{p_0}\right)$.

Case 2: $\alpha^2 - 4\beta < 0$

$$\phi_1(\xi) = \pm\sqrt{2}\left(-\frac{\alpha}{2}\right.$$
$$\left.+ \gamma\left(\frac{-c_1 \sin\left[\gamma\left(\frac{x^\lambda}{\lambda} - c\frac{t^\mu}{\mu}\right)\right] + c_2 \cos\left[\gamma\left(\frac{x^\lambda}{\lambda} - c\frac{t^\mu}{\mu}\right)\right]}{c_1 \cos\left[\gamma\left(\frac{x^\lambda}{\lambda} - c\frac{t^\mu}{\mu}\right)\right] + c_2 \sin\left[\gamma\left(\frac{x^\lambda}{\lambda} - c\frac{t^\mu}{\mu}\right)\right]}\right)\right) + p_0,$$

$$\phi_2(\xi) = \pm\sqrt{\frac{2}{\delta}}\left(-\frac{\alpha}{2}\right.$$
$$\left.+ \gamma\left(\frac{-c_1 \sin\left[\gamma\left(\frac{x^\lambda}{\lambda} - c\frac{t^\mu}{\mu}\right)\right] + c_2 \cos\left[\gamma\left(\frac{x^\lambda}{\lambda} - c\frac{t^\mu}{\mu}\right)\right]}{c_1 \cos\left[\gamma\left(\frac{x^\lambda}{\lambda} - c\frac{t^\mu}{\mu}\right)\right] + c_2 \sin\left[\gamma\left(\frac{x^\lambda}{\lambda} - c\frac{t^\mu}{\mu}\right)\right]}\right)\right) + \frac{p_0}{\sqrt{\delta}},$$

$$(2.24)$$

where $\gamma = \frac{\sqrt{4\beta - \alpha^2}}{2}$, and $c = \pm\frac{1}{\sqrt{2}}\left(2r - 3p_0 + \frac{6\beta}{p_0}\right)$.

Case 3: $\alpha^2 - 4\beta = 0$

$$\phi_1(\xi) = \pm\sqrt{2}\left(\frac{c_2}{c_1 + c_2\left(\frac{x^\lambda}{\lambda} - c\frac{t^\mu}{\mu}\right)} - \frac{\alpha}{2}\right) + p_0,$$
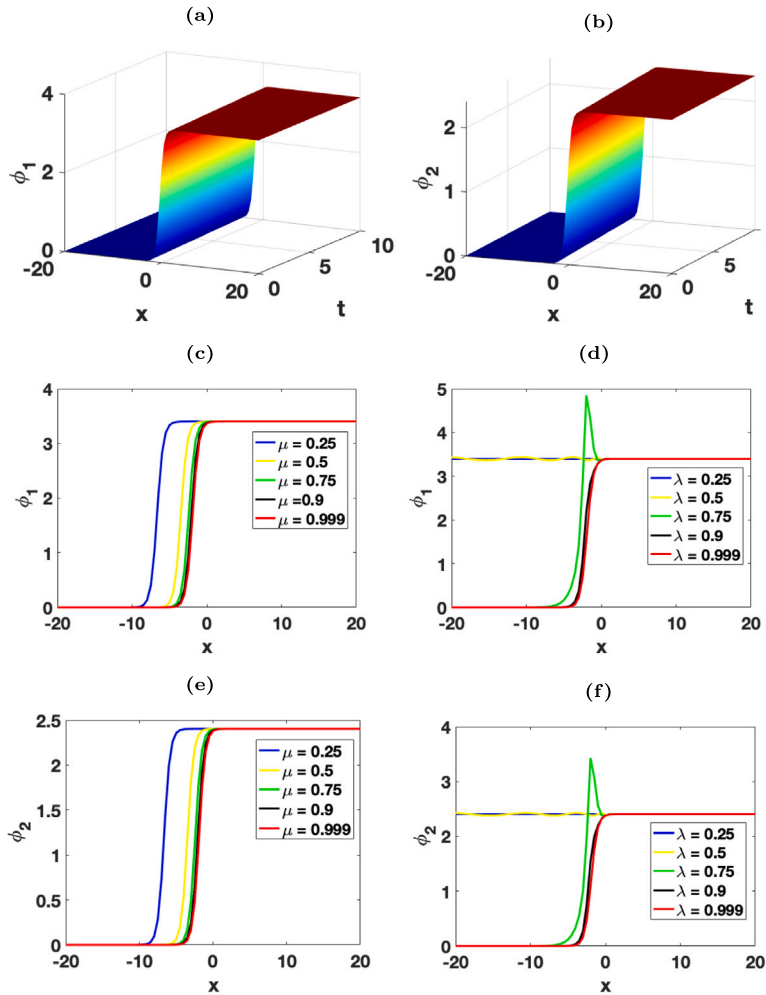
(a)

(b)

(c)

(d)

(e)

(f)

Fig. 4. Density distribution of prey (ϕ_1) and predator (ϕ_2) using the kink-like solution (2.23) for (2.2). For $\mu = 1$ and $\lambda = 1$, (a) prey density; (b) predator density. (c) and (e) prey and predator densities for various μ, (d) and (f) prey and predator densities for various λ at $t = 1$. The other parameters are $p_0 = 5$, $c_1 = 0.2$, $c_2 = 0.5$, $\beta = 4$, $\delta = 2$ and $r = 3$.

$$\phi_2(\xi) = \pm \sqrt{\frac{2}{\delta}} \left(\frac{c_2}{c_1 + c_2 \left(\frac{x^\lambda}{\lambda} - c \frac{t^\mu}{\mu} \right)} - \frac{\alpha}{2} \right) + \frac{p_0}{\sqrt{\delta}}. \qquad (2.25)$$

where $p_0 = \sqrt{2\beta}$, and $c = \pm \frac{1}{\sqrt{2}} \left(2r - 3p_0 + \frac{6\beta}{p_0} \right)$.

We proceed to discuss the characteristics of the second set of solitary waves by examining the solutions provided in Eqs. (2.23)–(2.25) for the CSTFDPP model (2.2). Figs. 4(a)–(b) illustrate the fundamental features of the kink-type solitary wave profiles for prey and predator density using the solution (2.23) with $\lambda = \mu = 1$. From a biological perspective, these profiles can be interpreted as both population densities experiencing a sudden increase and reaching a saturation level. By varying the time and space-fractional derivative parameters in (2.23), different dynamical properties in prey and predator densities are observed. For instance, when $\lambda = 0.99$ is fixed, and μ varies from 0 to 1, distinct propagation features of the kink solitary wave profile for prey density are depicted in Figs. 4(c) and (e). Additionally, a noticeable phase shift in the density profiles is observed when altering the value of μ from 0.25 to 0.999. Furthermore, when μ is held constant at 0.99 and λ is varied from 0.25 to 0.7, the resulting profiles become almost flattened, and as λ approaches 1, a kink-like solitary wave profile emerges. This observation is illustrated in Figs. 4(d) and 4(f) for prey and predator population density, respectively.

The density profiles for prey and predator populations, depicted in Fig. 5, are plotted as functions of time and spatial fractional derivative powers utilizing the solution (2.24). In Figs. 5(a)–(b), the usual periodic wave features are observed for prey and predator density when $\mu = \lambda = 1$. Variations in the periodic profile for prey density are illustrated in Figs. 5(c) and 5(e) by manipulating the time fractional derivative power. Similarly, changes in the predator density profile or periodic wave are noted by adjusting the space fractional derivative power parameter λ, as shown in Figs. 5(d) and 5(f).

Fig. 6 presents the qualitative nature of rational-type solitary wave profiles for prey and predator populations using the rational solution provided in (2.25). For the settings $\lambda = \mu = 1$, the corresponding density profiles for prey and predator are displayed in Figs. 6(a) and 6(b), respectively. Variations in the rational solitary wave profile are observed when adjusting the space and time fractional derivative powers, as shown in Figs. 6(c)–6(f).

3. Conclusion

In this work, we have constructed solitary wave solutions for the conformable fractional space–time diffusive predator–prey system. We have transformed the fractional model into its counterpart in the integer model by employing fractional derivative wave transformation. Using the $\left(\frac{G'}{G} \right)$ expansion method, we have obtained three different
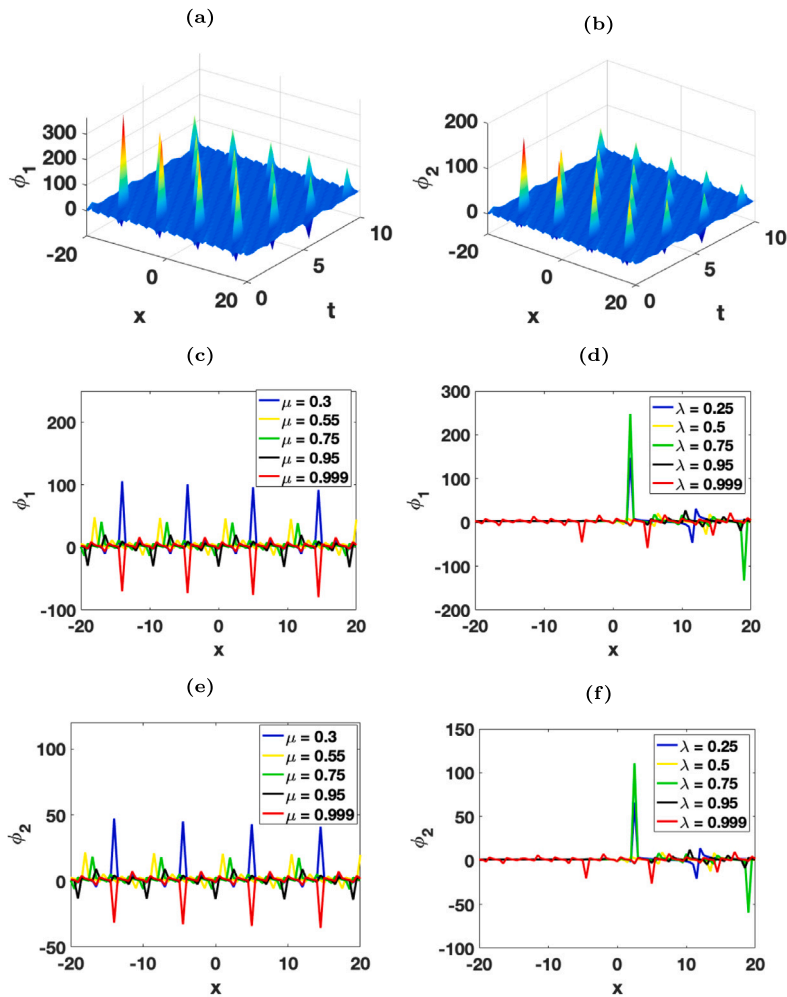
Fig. 5. Density distribution of prey (ϕ_1) and predator (ϕ_2) using the solution (2.24) for (2.2). For time and space fractional parameter $\mu = 1$ and $\lambda = 1$, (a) prey density; (b) predator density. (c) and (e) prey and predator densities for various μ, (d) and (f) prey and predator densities for various λ at $t = 1$. The other parameters are $p_0 = 5$, $c_1 = 0.15$, $c_2 = 2.1$, $\beta = 4$ and $r = 3.65$.

solitary wave solutions, namely kink-type, periodic, and rational, for two different cases for the transformed two coupled ordinary differential equations. By substituting these constructed solutions into the fractional derivative wave transformation, we have deduced the space–time fractional solitary wave solutions. We have then analyzed the various characteristics of prey and predator densities by tuning the space and time fractional order parameters/derivative powers. Our results reveal that when we fix the space and time-fractional derivative powers to unity, we observe the fundamental characteristics of solitary wave profiles. Additionally, we have observed phase shifts, singularities, and variations in the amplitude in the density profiles. These findings can carry significant implications for understanding population dynamics in ecological systems and for developing effective control strategies.

The methods presented in this paper can be applied to investigate other NFPDEs, specifically the new (3+1)-dimensional fractional fourth-order nonlinear equation, the (2+1)-dimensional Boussinesq equation, and the (3+1)-dimensional Kudryashov–Sinelshchikov equation. This involves utilizing classical soliton molecules solutions of these equations, which have been constructed in Refs. 49–51. The outcomes are anticipated to offer new insights and inspiration for the advancement of fractal theory in physics. Moreover, as a potential avenue for future research, the current theoretical study can be

readily extended to explore higher-order solitons, breathers, and rogue waves.[52–54] This extension would involve considering combined spatial and longitudinally varying dispersion and nonlinear effects, as well as introducing new forms of PT-symmetric potentials. This broader investigation aims to unveil potential applications in optical systems.

Declaration of competing interest

The authors declare that they have no known competing financial interests or personal relationships that could have appeared to influence the work reported in this paper.

Data availability

No data was used for the research described in the article.

(a)   (b)

(c)   (d)

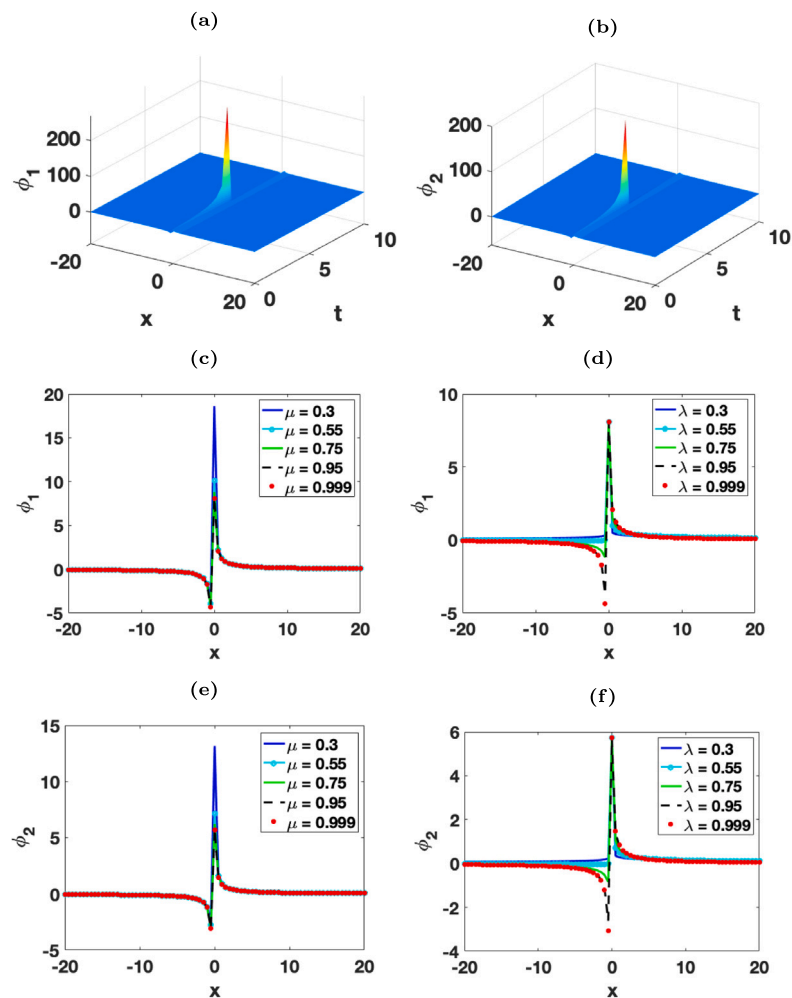(e)   (f)

Fig. 6. Density distribution of prey (ϕ_1) and predator (ϕ_2) using the rational solution (2.25) for (2.2). For time and space fractional parameter $\mu = 1$ and $\lambda = 1$, (a) prey density; (b) predator density. (c) and (e) prey and predator densities for various μ, (d) and (f) prey and predator densities for various λ at $t = 1$. The other parameters are $c_1 = 1.25$, $c_2 = 5.75$, $\mu = 1.5$, $\delta = 2$ and $k = 0.03$.

References

1. Murray JD. *Mathematical Biology*. Berlin: Springer; 2001.
2. Okubo A, Levin SA. *Diffusion and Ecological Problems*. New York: Springer; 2001.
3. Petrovskii SV, Li BL. *Exactly Solvable Models of Biological Invasion*. New York: Chapman & Hall/CRC; 2006.
4. Petrovskii SV, Malchow H, Li BL. An exact solution of a diffusive predator–prey system. *Proc R Soc Lond Ser A Math Phys Eng Sci*. 2005;461:1029–1053.
5. Kraenkel RA, Manikandan K, Senthilvelan M. On certain new exact solutions of a diffusive predator–prey system. *Commun Nonlin Sci Num*. 2013;18:1269–1274.
6. Tang B. Dynamics for a fractional-order predator–prey model with group defense. *Sci Rep*. 2020;10:4906.
7. Ghanbari B, Kumar D. Numerical solution of predator–prey model with Beddington–deAngelis functional response and fractional derivatives with Mittag-Leffler kernel. *Chaos: Interdiscip J Nonlinear Sci*. 2019;29:063103.
8. Baisad K, S. Moonchai S. Analysis of stability and hopf bifurcation in a fractional Gauss-type predator–prey model with allee effect and Holling type-III functional response. *Adv Differential Equations*. 2018;2018:82.
9. Yavuz M, Sulaiman TA, Yusuf A, Abdeljawad T. The Schrödinger-KdV equation of fractional order with Mittag-Leffler nonsingular kernel. *Alex Eng J*. 2021;60:2715.
10. Evangelista LR, Lenzi EK. *Fractional Diffusion Equations and Anomalous Diffusion*. Cambridge University Press; 2018.
11. Tamm MV, Nazarov LI, Gavrilov AA, Chertovich AV. Anomalous diffusion in fractal globules. *Phys Rev Lett*. 2015;114:178102.
12. Fagan WF, Lewis MA, Neubert MG, van den Driessche P. Invasion theory and biological control. *Ecol Lett*. 2002;5:148–157.
13. Frantzen J, van den Bosch F. Spread of organisms: can travelling and dispersive waves be distinguished? *Basic Appl Ecol*. 2000;1:83–91.
14. Sasmal SK, Anshu Dubey B. Diffusive patterns in a predator–prey system with fear and hunting cooperation. *Eur Phys J Plus*. 2022;137:281.

15. Souna F, Djilali S, Alyobi S, et al Spatiotemporal dynamics of a diffusive predator–prey system incorporating social behavior. *AIMS Math*. 2023;8:15723–15748.
16. Ali M, Alquran M, Jaradat I. Explicit and approximate solutions for the conformable-Caputo time-fractional diffusive predator-prey model. *Int J Appl Comput Math*. 2021;7:90.
17. Ghanbari B, Nisar KS, Aldhaifallah M. Abundant solitary wave solutions to an extended nonlinear Schrödinger's equation with conformable derivative using an efficient integration method. *Adv Differential Equations*. 2020;1:25.
18. Mezouaghi A, Djilali S, Bentout S, Biroud K. Bifurcation analysis of a diffusive predator–prey model with prey social behavior and predator harvesting. *Math Methods Appl Sci*. 2022;45:718–731.
19. Djilali S, Bentout S, Zeb A. Dynamics of a diffusive delayed viral infection model in a heterogeneous environment. *Math Methods Appl Sci*. 2023;46:16596–16624.
20. Djilali S. Threshold asymptotic dynamics for a spatial age-dependent cell-to-cell transmission model with nonlocal disperse. *Discrete Contin Dyn Syst B*. 2023;28:4108–4143.
21. Longhi S. Fractional Schrödinger equation in optics. *Opt Lett*. 2015;40:1117.
22. Laskin N. Fractional Schrödinger equation. *Phys Rev E*. 2002;66:056108.
23. Chen W, Sun H, Zhang X, Korosak D. Anomalous diffusion modeling by fractal and fractional derivatives. *Comput Math Appl*. 2010;59:1754–1758.
24. Mahmud Shahen NH, Foyjonnesa, Shuzon Ali Md, Mamun AA, Rahman MM. Interaction among lump, periodic, and kink solutions with dynamical analysis to the conformable time-fractional Phi-four equation. *Partial Differ Equ Appl Math*. 2021;4:100038.
25. He JH. A tutorial review on fractal space–time and fractional calculus. *Internat J Theoret Phys*. 2014;53:3698–3718.
26. He JH. Fractal calculus and its geometrical explanation. *Results Phys*. 2018;20:272–276.
27. Lu B. The first integral method for some time fractional differential equations. *J Math Anal Appl*. 2012;395:684–693.

28. Tong B, He Y, Wei L, Zhang X. A generalized fractional sub-equation method for fractional differential equations with variable coefficients. *Phys Lett A*. 2012;376:2588–2590.

29. Zhang S, Zong QA, Liu D, Gao Q. A generalized exp-function method for fractional riccati differential equations. *Commun Fract Calc*. 2010;1:48–51.

30. Manikandan K, Aravinthan D, Sudharsan JB, Reddy SRR. Soliton and rogue wave solutions of the space–time fractional nonlinear Schrödinger equation with $\mathcal{PT}$-symmetric and time-dependent potentials. *Optik*. 2022;266:169594.

31. Nur Alam MD. An analytical technique to obtain traveling wave solutions to nonlinear models of fractional order. *Partial Differ Equ Appl Math*. 2023;8:100533.

32. Devnath S, Khan K, Ali Akbar M. Numerous analytical wave solutions to the time-fractional unstable nonlinear Schrödinger equation with beta derivative. *Partial Differ Equ Appl Math*. 2023;8:100537.

33. Yavuz M, Sene N. Stability analysis and numerical computation of the fractional predator–prey model with the harvesting rate. *Fractal Fract*. 2020;4:35.

34. Mohan L, Prakash A. Stability and numerical analysis of the generalised time-fractional cattaneo model for heat conduction in porous media. *Eur Phys J Plus*. 2023;138:294.

35. Wang BH, Wang YY, Dai CQ, Chen YX. Dynamical characteristic of analytical fractional solitons for the space–time fractional fokas-lenells equation. *Alex Eng J*. 2020;59:4699–4707.

36. Manafian J, Ilhan OA, Avazpour L. The extended auxiliary equation mapping method to determine novel exact solitary wave solutions of the nonlinear fractional PDEs. *Int J Nonlinear Sci Numer*. 2021;22:69–82.

37. Manikandan K, Aravinthan D, Sudharsan JB, Vadivel R. Optical solitons in the generalized space–time fractional cubic-quintic nonlinear Schrödinger equation with a $\mathcal{PT}$-symmetric potential. *Optik.*. 2022;271:170105.

38. Vinodbhai CD, Dubey S. Investigation to analytic solutions of modified conformable time–space fractional mixed partial differential equations. *Partial Differ Equ Appl Math*. 2022;5:100294.

39. Khalil R, Al Horani M, Yousef A, Sababheh M. A new definition of fractional derivative. *J Comput Appl Math*. 2014;264:65–70.

40. Atangana A, Baleanu D, Alsaedi A. New properties of conformable derivative. *Open Math*. 2015;13:1–10.

41. Chen W. Time-space fabric underlying anomalous diffusion. *Chaos Solitons Fractals*. 2006;28:923–929.

42. Zheng B, Kai Y, Xu W, Yang N, Zhang K. Exact traveling and non-traveling wave solutions of the time fractional reaction–diffusion equation. *Physica A*. 2019;532:121780.

43. Wang KJ, Xu P, Shi F. Nonlinear dynamic behaviors of the fractional (3+1)-dimensional modified Zakharov-Kuznetsov equation. *Fractals*. 2023;31:2350088.

44. Wang KJ, Xu P. Generalized variational structure of the fractal modified KdV-Zakharov-Kuznetsov equation. *Fractals*. 2023;31:2350084.

45. Wang KJ. New exact solutions of the local fractional modified equal width-Burgers equation on the cantor sets. *Fractals*. 2023;31:2350111.

46. Poonia M, Singh K. Exact traveling wave solutions of diffusive predator prey system using the first integral method. *AIP Conf Proc*. 2020;2214:020027.

47. Abdelrahman M, Zahran E, Khater M. The $\exp(-\varphi(\zeta))$-expansion method and its application for solving nonlinear evolution equations. *Int J Mod Nonlinear Theory Appl*. 2015;4:37–47.

48. Zayed EM, Amer YA. The modified simple equation method for solving nonlinear diffusive predator–prey system and Bogoyavlenskii equations. *Int J Phys Sci*. 2015;10:133–141.

49. Wang KJ. Soliton molecules, interaction and other wave solutions of the new (3+1)-dimensional integrable fourth-order equation for shallow water waves. *Phys Scr*. 2024;99:015223.

50. Wang KJ. Soliton molecules and other diverse wave solutions of the (2+1)-dimensional Boussinesq equation for the shallow water. *Eur Phys J Plus*. 2023;138:891.

51. Wang KJ. Dynamics of complexiton, γ-type soliton and interaction solutions to the (3+1)-dimensional Kudryashov-Sinelshchikov equation in liquid with gas bubbles. *Results Phys*. 2023;54:107068.

52. Alquran M, Sulaiman TA, Yusuf A, Alshomrani AS, Baleanu D. Nonautonomous lump-periodic and analytical solutions to the (3+1)-dimensional generalized Kadomtsev–Petviashvili equation. *Nonlinear Dynam*. 2023;111:11429–11436.

53. Atas SS, Ismael HF, Sulaiman TA, Bulut H. Investigation of some nonlinear physical models: exact and approximate solutions. *Opt Quantum Electron*. 2023;55:293.

54. Ibrahim S, Baleanu D. Classes of solitary solution for nonlinear Schrödinger equation arising in optical fibers and their stability analysis. *Opt Quantum Electron*. 2023;55:1158.